ELSEVIER

Journal of Alloys and Compounds 239 (1996) 203–208

Journal of ALLOYS AND COMPOUNDS

Ti_5C_4 phase formation in rapidly solidified $Al_{96.52}Fe_{2.03}Si_{0.64}Ti_{0.46}C_{0.35}$ alloy

X.C. Tong, H.S. Fang, B.C. Liu

Department of Materials Science and Engineering, Tsinghua University, Beijing 100084, People's Republic of China

Received 9 November 1995; in final form 17 December 1995

Abstract

The as-solidified and annealed microstructures of a rapidly solidified $Al_{96.52}Fe_{2.03}Si_{0.64}Ti_{0.46}C_{0.35}$ alloy were evaluated. The as-solidified microstructure comprised an intracellular uniform, fine-scale dispersion of Al_6Fe phase in α-Al and elongated amorphous particles located along the cell boundaries, with approximately 0.46 at.% Ti and 0.35 at.% C saturated in the α-Al. During annealing, the amorphous phase transformed into α_T-AlFeSi phase, and some of the Al_6Fe dispersoids increased in size while others were replaced by Al_3Fe particles. After annealing at 773 K for 5 h, face centered cubic TiC particles, of approximate atomic composition Ti_5C_4 and lattice parameter 0.424 nm, precipitated in the α-Al matrix. Moreover, there is a cube–cube orientation relationship between Ti_5C_4 and the α-Al matrix with a disregistry of $\delta = 0.05$. The formation mechanism of this TiC is discussed.

Keywords: Titanium carbide; Rapid solidification; Precipitation; Formation; TEM

1. Introduction

Recently, development of high-temperature aluminum alloy for structural applications has been mainly focused on dispersion of strengthening, for which a desirable microstructure consists of a high volume fraction of evenly distributed fine, hard intermetallic phase particles with low coarsening rates, which is generally favored by low interfacial energy of the intermetallic phase in the aluminum matrix. Rapidly solidified (RS) Al–Fe is an attractive system, owing to the production of fine dispersoids that exhibit unusually low coarsening rates, and has become the basis for most of the high-temperature aluminum alloys developed to date, e.g. Al–Fe–X (X = Cr, Mo, Zr, V + Si, Ce and W etc.) [1,2]. If a dispersed TiC phase could form directly in the Al–Fe system by adding Ti and C, a new alloy system of Al–Fe/TiC would be of interest in engineering applications. This is because the TiC phase itself has high values of strength and hardness, very high melting point and superior thermal stability. This paper reports the microstructural characteristics of the RS $Al_{96.52}Fe_{2.03}Si_{0.64}Ti_{0.46}C_{0.35}$ alloy and phase transformations during its annealing, especially the TiC formation in this alloy.

2. Experimental

The $Al_{96.52}Fe_{2.03}Si_{0.64}Ti_{0.46}C_{0.35}$ alloy bars were prepared from 99.9% Al, 99.7% Ti, 99.7% Si, medium carbon steel and graphite particles about 1 mm average particle size by vacuum induction melting under argon in a graphite crucible and chill-casting in a cast iron mold. RS samples were prepared by chill block melt-spinning. An alloy charge of about 20 g was remelted in a quartz crucible under a flowing Ar atmosphere, using a calibrated pyrometer to monitor alloy temperature. After holding at 1673 K for 5 min, the molten alloy was ejected with an Ar overpressure of 60 kPa onto the outer surface of a copper drum rotating with a surface linear velocity of 30 m s^{-1}. The ribbons obtained were approximately 5 mm wide and 40 to 50 μm thick. Sections of the ribbon were subsequently heat-treated in a graphite powder bath at 773 K for 5 h to examine phase transformations during annealing. The specimen for transmission electron microscopy (TEM) were prepared firstly by jet electropolishing and ion milling. TEM examination was performed in a Jeol-2000FX transmission electron microscope equipped with a Link AN-10000 energy dispersive X-ray spectrometer (EDS). Electron energy loss spectrum (EELS) analysis was carried out in a

PII S0925-8388(96)02234-7

Philips CM12 transmission electron microscope interfaced to a GATAN666 facility, using the P absorption edge. During the quantitative microanalysis by EDS and EELS, calibration with a standard sample was carried out.

3. Results and discussion

Fig. 1 shows that the as-solidified microstructure consists of α-Al cells, from 0.15 to 0.30 μm in size, with intra- and intercellular intermetallic particles of average size 10 to 50 nm. The globular intracellular particles were determined to be the Al_6Fe metastable phase structure (Fig. 1(c)). Intercellular particles which were more elongated had an amorphous structure (Figs. 1(c) and 1(d)); EDS analysis indicated that this amorphous phase had a composition of 66.9 wt.% Al, 27.9 wt.% Fe and 5.2 wt.% Si (note that its Fe content is slightly higher than that of Al_6Fe, 25.6 wt.% Fe, see Figs. 1(e) and 1(f)). Previous work [3,4] showed that the amorphous phase is not a 'normal' metallic glass (dense random packing model) but probably similar to that observed in binary Al–Fe and called 'S' phase by Shechtman and Swartzendruber [5]. Meanwhile, no Ti- or C-enriched phases were found, and EDS and EELS

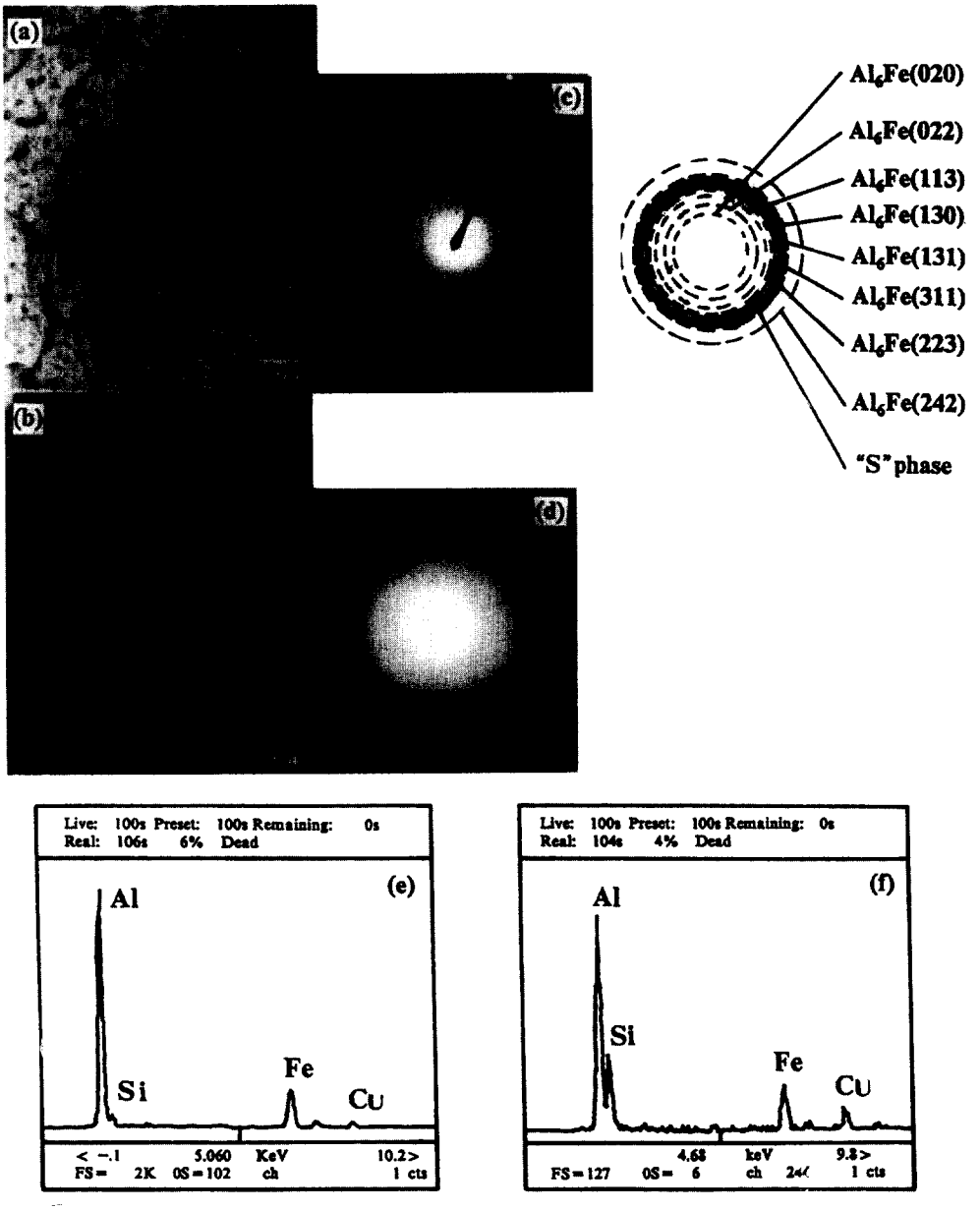

Fig. 1. TEM bright-field (a) and dark-field (b) images, and corresponding selected area diffraction pattern (c) and microdiffraction pattern from elongated particles along cell boundaries (d). Energy dispersive X-ray spectra from the globular Al_6Fe phase (e) and the elongated 'S' phase (f). Also shown are the positions of the objective area aperture and the identified individual reflections from the α-Al matrix, diffuse rings from amorphous elongated phase, and spotty rings from particles of the globular Al_6Fe phase; (c) confirms the amorphous structure of the 'S' phase.

analyses confirmed that the Ti and C contents (Fig. 2) of the α-Al were close to those of the nominal alloy composition of 0.46 at.% and 0.35 at.% respectively.

During annealing at 773 K for 5 h, the α-Al cells grew to 0.6 ± 0.1 μm while the intermetallic phase particles were replaced by much coarser polygonal particles (transformed from the amorphous phase, marked A), needle-like particles (marked B) and globular particles (from the globular Al_6Fe dispersoids, marked C); these were respectively indexed as α_T-AlFeSi (C-centered monoclinic, $a = 2.795$ nm, $b = 3.062$ nm, $c = 2.073$ nm, $\beta = 97.74°$ [6]), Al_3Fe (C-centered monoclinic, $a = 1.549$ nm, $b = 0.808$ nm, $c = 2.703$ nm, $\beta = 107.75°$ [6]) and Al_6Fe (C-centered orthorhombic, $a = 0.649$ nm, $b = 0.744$ nm, $c = 0.879$ nm [6]), as shown in Fig. 3. Furthermore, much smaller particles precipitate on the α-Al matrix, identified as a TiC phase (marked in Fig. 3(a)) by microdiffraction, with a lattice parameter of 0.424 nm (Fig. 4). EELS analysis indicated the atomic composition to be Ti_5C_4 (Fig. 5), corresponding to the nominal atomic composition C:Ti = 0.76. This shows that the alloying element Ti formed mostly as Ti_5C_4; excess Ti was probably present in the Al_3Fe or Al_6Fe particles, or retained in supersaturated solid solution in the α-Al matrix to some extent. Moreover, the microdiffraction analysis (Fig. 4) of the α-Al matrix near the approximate Ti_5C_4 phase showed that a cube–cube orientation relationship was present between Ti_5C_4 and the α-Al matrix, and that the disregistry δ between Ti_5C_4 and α-Al could be calculated as $\delta = (0.0424 - 0.4030)/0.0424 = 0.05$, showing that the Ti_5C_4 phase has a coherent or near-coherent interface with the α-Al matrix.

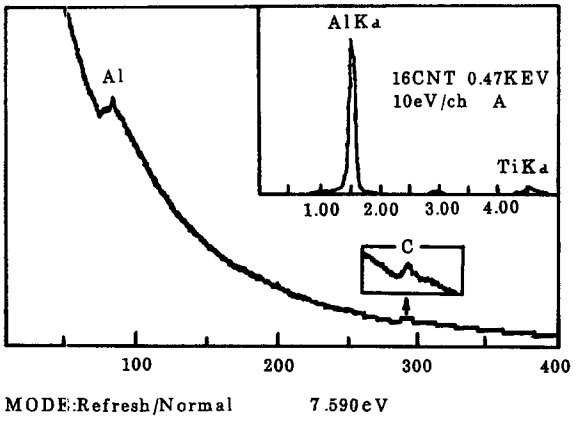

Fig. 2. EELS analysis data of Ti and C contents inside α-Al matrix.

In the Al–Fe alloy, the amorphous phase formation has been explained in previous work [3,5] as arising from either liquid-phase separation, first-order transformation, or Al 'S' phase eutectic growth. Among these explanations, the most preferred to the authors is the amorphous phase formation by Al–'S' phase

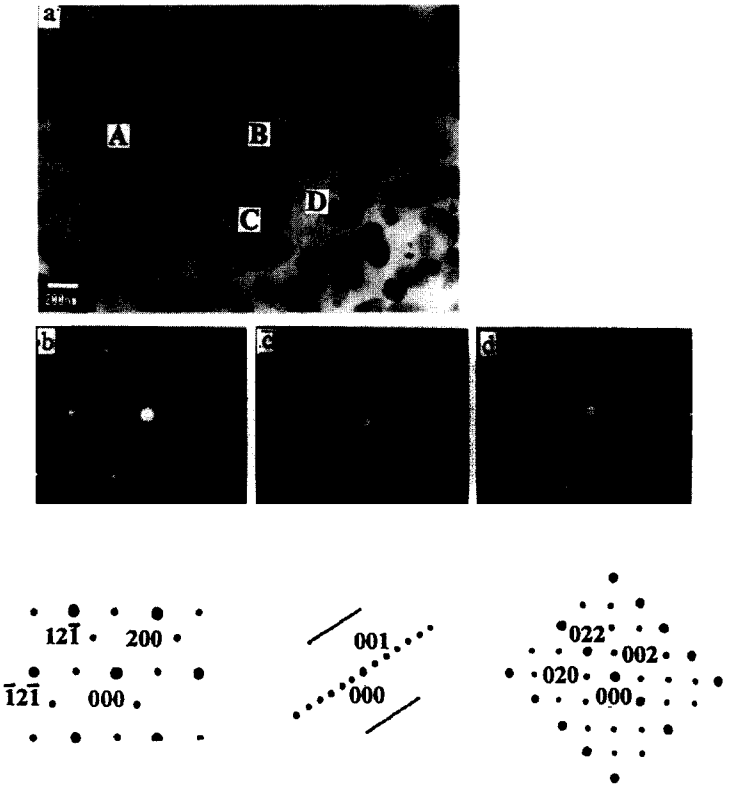

Fig. 3. (a) Microstructure of the alloy annealed at 773 K for 5 h; (b), (c), (d) are diffraction patterns of α_T-AlFeSi, Al_3Fe and Al_6Fe respectively.

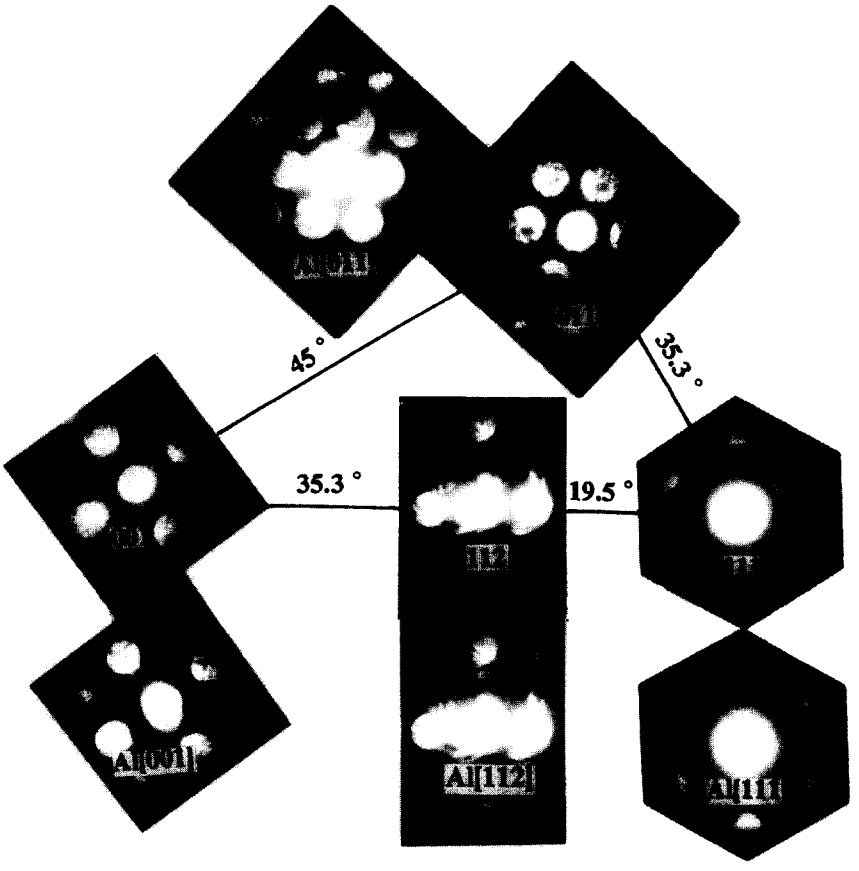

Fig. 4. A series of microdiffraction patterns from the approximate Ti_3C_4 phase and α-Al matrix within the unit stereographic triangle.

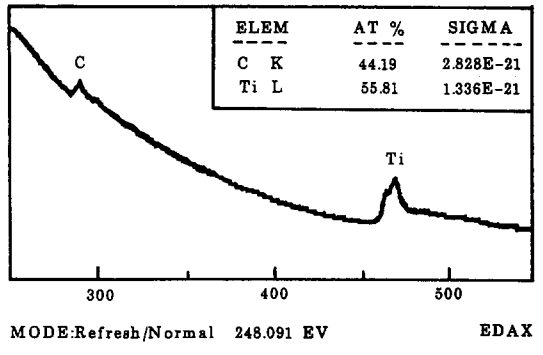

Fig. 5. EELS analysis data of the approximate Ti_3C_4 phase.

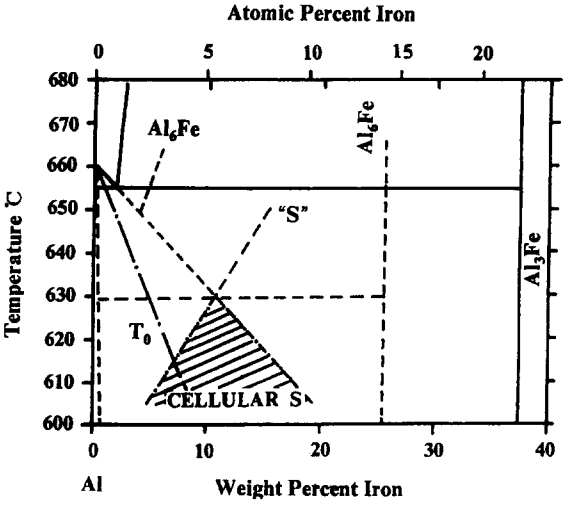

Fig. 6. A hypothetical metastable phase diagram for Al-rich aluminum–iron alloy showing the approximate location of the metastable 'S' phase eutectic between α-Al solid solution and the Al_6Fe composition of the 'S' phase (Fe content).

degenerate eutectic growth during extremely rapid solidification, i.e. such a high undercooling is reached (at least below the T_0 temperature of Al–Fe) that rapid solidification of the alloy would have happened in the temperature range of Al–'S' phase coupled growth eutectic regions (Fig. 6). The α-Al initially nucleated homogeneously and grew with extensive solute trapping of Fe, Ti and C elements, followed by coupled growth of the 'S' phase. During recoalescence, the Al_6Fe precipitated in the α-Al supersaturation. In the annealed microstructure, the 'S' phase transformed into α_T-AlFeSi phase with a composition near that of the 'S' phase.

In order to explain the TiC phase formation, the following reaction will be analyzed:

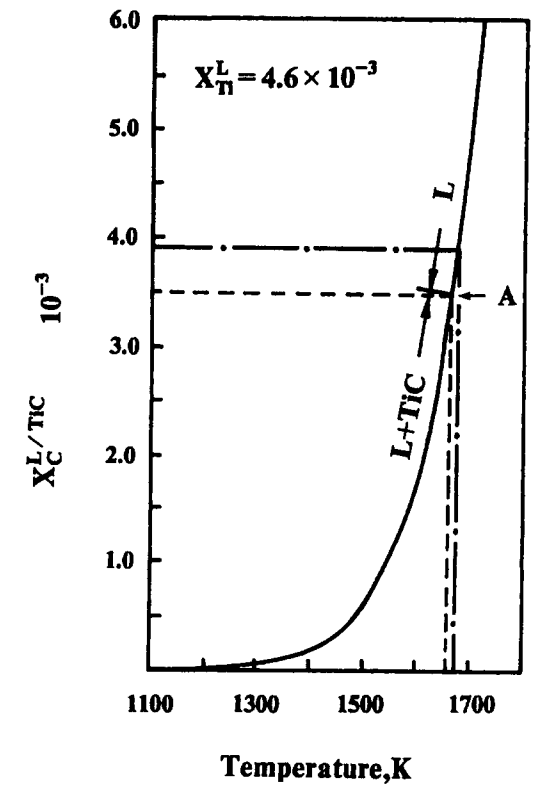

Fig. 7. The stability diagram for Ti in the Al–Ti–C system.

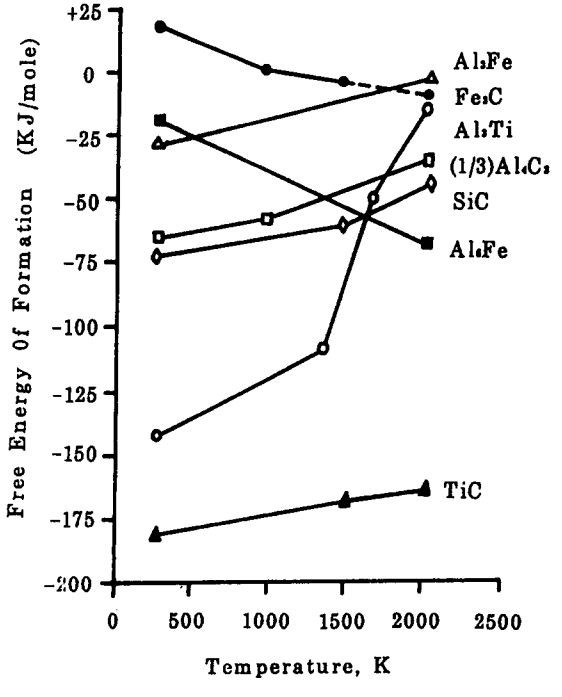

Fig. 8. Free energy of formation ΔG^0 as a function of temperature for Fe_3C, SiC, TiC and $(1/3)Al_4C_3$ (data from Ref. [8]) as well as Al_6Fe, Al_3Fe (data from Ref. [9]) and Al_3Ti (data from Refs. [7] and [10]).

$$Ti + C = TiC(s) \quad (1)$$

where Ti and C are solutes in the aluminum solution. The change of free energy can be written as

$$\Delta G_{TiC} = \Delta G^0_{TiC} + RT\ln[a_{TiC}/(a_{Ti}a_C)] \quad (2)$$

Assuming that Raoult's law is valid for carbon and titanium, at equilibrium the following is obtained:

$$\gamma^0_C X^{L/TiC}_C \gamma^0_{Ti} X^L_{Ti} = \exp[\Delta G^0_{TiC}/(RT)] \quad (3)$$

The values for ΔG^0_{TiC} and γ^0_C and γ^0_{Ti} can be found in Ref. [7], so that the following expressions are obtained:

$$X^{L/TiC}_C = \exp(5.1298 - 26865.472/T)/X_{Ti}$$

where $X^{L/TiC}_C$ is the mole fraction of carbon in liquid Al in equilibrium with TiC, and X_{Ti} is the mole fraction of titanium in liquid Al.

This expression is presented in a diagrammatic form in Fig. 7 for $X_{Ti} = 4.6\times10^{-3}$. For the present alloy, $X_C = 3.5\times10^{-3}$, corresponding to the temperature 1660 K. This is the critical point (marked A in Fig. 7) at which the alloy elements Ti and C can be completely dissolved in liquid aluminium to equilibrate with TiC. Since the superheating temperature 1673 K (corresponding to $X_C = 3.9\times10^{-3}$) of the alloy before quenching is higher than the critical point temperature 1660 K, the alloy elements Ti and C completely dissolve in the liquid aluminum before quenching. At a very large undercooling, the high growth velocity is large enough to result in the trapping state of Ti and C in the α-Al, where they remain to room temperature after quenching. During the annealing at 773 K for 5 h, the Ti_5C_4 phase precipitated on the α-Al matrix. This could be thermodynamically interpreted by Fig. 8, which compares the formation free energy as a function of temperature for Al_6Fe, Al_3Fe and Al_3Ti as well as Al_4C_3, SiC and TiC on a per mole of carbon basis. On this basis, the formation of all these phases is possible. However, TiC has a substantially lower formation free energy than the other phases over the full range of temperature up to 2073 K. Therefore, both in the liquid state and in the solid state of the alloy the formation of TiC should always be favorable.

References

[1] S. Mitra and T.R. McNelley, *Metall. Trans. A, 24* (1993) 2589.
[2] M.K. Premkumar, A. Lawley and M.J. Koczak, *Metall. Trans. A, 23* (1992) 3219.
[3] J.A. Bendersy, F.S. Biancaniello and R.J. Schaefer, *J. Mater. Res., 2* (1987) 427.
[4] L.A. Bendersky, A.J. McAlister and F.S. Biancaniello, *Metall. Trans. A, 19* (1988) 2893.

[5] D. Shechtman and L.J. Swartzendruber, in L.H. Bennett, T.B. Massalski and B.C. Giessen (eds.), *Alloy Phase Diagrams*, Elsevier, New York, 1983, p. 265.
[6] P. Skjerpe, *Metall. Trans. A, 18* (1987) 189.
[7] A. Jarfors and H. Fredriksson, *Microgravity Sci. Technol., III* (4) (1991) 216.
[8] E.A. Brands (ed.), *Smithells Metals Reference Book*, Butterworth, 1983.
[9] J.L. Murray, in L.H. Bennett, T.B. Massalski and B.C. Giessen (eds.), *Alloy Phase Diagrams*, Elsevier, New York, 1983, p. 249.
[10] J.L. Murray, *Metall. Trans. A, 19* (1980) 243.